CAGE: Software for a Critical Analysis of ^{2}H Spin−Lattice Relaxation in Liquid Crystals

Lucia Calucci[†] and Marco Geppi*[,#]

Istituto di Chimica Quantistica ed Energetica Molecolare, CNR, Area della Ricerca di Pisa, via V. Alfieri 1, 56010, San Giuliano Terme, Pisa, Italy, and Dipartimento di Chimica e Chimica Industriale, Università degli Studi di Pisa, via Risorgimento 35, 56126, Pisa, Italy

Received December 27, 2000

A software package of Mathematica, aimed at the analysis of ^{2}H NMR Zeeman (T_{1Z}) and quadrupolar (T_{1Q}) spin−lattice relaxation times in liquid crystals in terms of diffusional models, is presented. The models most commonly used to describe internal, overall, and collective motions in liquid−crystalline phases are considered, and dynamic parameters are obtained by means of either single point or global target approaches using simulation or fitting procedures. The use of the software as a tool for highlighting the problems encountered in this kind of analysis as well as for dealing with such problems following suitable strategies is illustrated by means of applications to experimental ^{2}H relaxation times of three different calamitic liquid crystals.

INTRODUCTION

The complex dynamics of thermotropic calamitic liquid crystals is characterized by a superposition of internal and overall molecular motions and collective fluctuations. Internal motions comprise reorientations such as trans−gauche chain isomerization and aromatic ring rotations, while two basic processes are distinguished for overall motions, namely rotation about the long molecular axis and reorientation of this axis. By using different techniques, the various motions can be studied over a wide dynamic range, extending from the fast (10^{-11} s) to the ultraslow (10 s) motional regime. Among them, ^{2}H spin−lattice relaxation has been established as a powerful tool for studying molecular dynamics in liquid crystalline phases in the range 10^{-11}−10^{-4} s.[1−4] The main advantage of ^{2}H NMR experiments on aligned liquid crystals is the relative simplicity of the spectra due to the dominant quadrupolar interaction. Because of this interaction each deuteron oriented differently with respect to a molecule fixed frame can be considered as an isolated spin-1 system and gives a doublet.

The most common relaxation experiments are measurements of the Zeeman spin−lattice relaxation time T_{1Z} and quadrupolar order decay time T_{1Q}, which can be obtained simultaneously by applying appropriate pulse sequences.[5,6] The Redfield theory directly relates the relaxation times to the spectral densities of motion (which are the Fourier transforms of the correlation functions) at the Larmor frequency and at twice this frequency. If detailed information on liquid crystal dynamics has to be obtained, it is necessary to measure as many individual spectral densities as possible. Spectral densities should be sampled as a function of temperature, frequency, and orientation of the phase director with respect to the external magnetic field. Moreover it is useful to monitor relaxation behavior of deuterons oriented differently with respect to the molecule fixed axes. The combination of these measurements requires a synthetic effort to obtain selectively deuterated samples, the avalaibility of suitable instrumentation, and long experimental times. Moreover, by increasing the number of deuterons, more complex spectra are obtained in which signal overlapping may complicate the extraction of individual relaxation times.[7]

After obtaining a set of relaxation data, the next step in determining motional information is the construction of models which lead to expressions of the correlation functions in terms of parameters characterizing the many different types of motion. Several models have been proposed to describe molecular reorientations, internal isomerizations, and collective motions in thermotropic calamitic liquid crystals.

The simplest model describes the overall molecular reorientation as isotropic *diffusion in a cone* characterized by a single coefficient.[8] A second rank diffusional tensor, which accounts for motional anisotropy, is considered in the model proposed by Nordio et al.[9] and in the *anisotropic viscosity* model.[10] Both models describe the reorientational motions of cylindrical molecules in uniaxial phases as small step diffusional rotation in a Maier-Saupe mean field potential. The diffusional tensor is diagonal in the principal molecular frame for the first model, while in the *anisotropic viscosity* model it is diagonal in a laboratory frame with its z axis along the phase director. Vold and Vold[11] extended the *anisotropic viscosity* model by introducing a third diffusional coefficient describing the rotation of the molecule around its long axis (*third rate anisotropic viscosity* model). Extensions of Nordio's model have been formulated by Tarroni and Zannoni[12] and by Berggren et al.[13] which apply to biaxial molecules in uniaxial phases and uniaxial molecules in biaxial phases, respectively.

Internal motions are usually considered decoupled from the overall molecular ones. Aromatic ring rotations have been

* Corresponding author phone: +39-050-918266; fax: +39-050-918260; e-mail: mg@dcci.unipi.it.
[†] Istituto di Chimica Quantistica ed Energetica Molecolare, CNR.
[#] Università degli Studi di Pisa.

10.1021/ci000169w CCC: $20.00
Published on Web 06/16/2001

described in an isotropic potential by means of either small step diffusion[14] or strong collision models[15] or in a 2-fold symmetric intramolecular potential considering coupled rotational isomerization and libration processes.[16] In the treatment of chain dynamics either stochastic rotational diffusion about C−C bonds or rotational jumps among equilibrium sites[17] may be considered; in turn, motions of different chain fragments can be taken as independent[18] or coupled.[19]

The contribution of order director fluctuations to spectral densities is usually expressed on the basis of the theories proposed by Pincus[20] and Blinc et al.[21]

A quantitative analysis of spectral densities, obtained from experimental ^{2}H spin−lattice relaxation times, in terms of diffusional models requires a fitting procedure where several parameters governing molecular and collective motions must be varied simultaneously, while geometrical (bond angles and lengths) and magnetic (quadrupolar coupling constants) parameters are usually fixed. Order parameters are determined from quadrupolar and dipolar splittings in the ^{2}H NMR spectra and introduced in the calculations where required. The number of dynamic parameters can increase dramatically as more sophisticated models are used, so that models of suitable complexity must be chosen on the basis of the number of experimental data. Nordio's and Volds' models for the description of overall motions are the most commonly reported in the literature, to which internal and collective motions are usually superimposed. The size of the experimental data set is of course related to the number of deuterons belonging to moieties oriented differently with respect to the long molecular axis. Nevertheless, a high number of deuterons causes several disadvantages in both the determination of relaxation times (vide supra) and the analysis of spectral densities. In fact, the introduction of deuterons in molecular fragments undergoing internal reorientations increases both experimental data and fitting parameters as well as computational complexity. To extend the experimental data set without increasing the number of deuterons, global target procedures[22] are often employed in which spectral densities measured at different temperatures are optimized together assuming an Arrhenius behavior for the diffusional coefficients.

Two main problems can rise when dealing with the fitting of deuterium relaxation data. First, the presence of strong correlations between parameters can prevent the extraction of single reliable optimized values, and, second, different sets of optimized parameters, with fits of similar quality, can be obtained depending on the initial values used.

The CAGE software has been written with the aim of critically investigating such problems, often disregarded in the papers published on this subject. This is a package of Mathematica[23] performing both simulation and fitting of deuterium spectral densities on the basis of different motional models, which makes available tools for both the calculation and graphical visualization of the results.

In the next section a theoretical description of the diffusive models included in the software is reported. This is followed by a section in which the facilities provided by the CAGE package are explained in detail. Some significant applications of the software to experimental data acquired in our research groups are presented in a separate section. Finally, in the last section, conclusions are drawn and extensions of the package are suggested.

DIFFUSIONAL MODELS

The following relationships link the spin−lattice relaxation times T_{1Z} and T_{1Q} to the spectral densities $J_1(\omega_0)$ and $J_2(2\omega_0)$:

$$\frac{1}{T_{1Z}} = J_1(\omega_0) + 4J_2(2\omega_0) \tag{1}$$

$$\frac{1}{T_{1Q}} = 3J_1(\omega_0) \tag{2}$$

where ω_0 is the Larmor frequency.

For a deuteron not involved in internal rotations, the spectral densities can be obtained as the Fourier transforms of the autocorrelation functions $g_{m_L m_M}(t)$, which, following Vold, are expressed as a sum of decreasing exponential functions:[11]

$$g_{m_L m_M}(t) = c_{m_L m_M} \sum_j a^{(j)}_{m_L m_M} \exp\left(-\frac{t}{\tau^{(j)}_{m_L m_M}}\right) \tag{3}$$

The following expression for J is obtained[4]

$$J_{m_L}(m_L\omega_0) = \frac{3\pi^2}{2}(\nu_q)^2 \sum_{m_M=-2}^{2} c_{m_L m_M}[d^2_{m_M 0}(\beta_{M,Q_0})]^2 \sum_j a^{(j)}_{m_L m_M} \times \frac{(\tau^{(j)}_{m_L m_M})^{-1}}{(m_L\omega_0)^2 + (\tau^{(j)}_{m_L m_M})^{-2}} \tag{4}$$

where ν_q is the quadrupolar coupling constant, d^2_{rs} are the reduced Wigner matrices, β_{M,Q_0} is the angle between the molecular long axis and the C−D bond of interest, $a^{(j)}_{m_L m_M}$ represent normalized relative weights of each exponential function with time constant $\tau^{(j)}_{m_L m_M}$, and $c_{m_L m_M}$ are the initial amplitudes of the correlation functions. The correlation times $\tau^{(j)}_{m_L m_M}$ are expressed in terms of diffusional coefficients on the basis of the following relationships, which hold for Nordio's (eq 5), *anisotropic viscosity* (eq 6), and Volds' (eq 7) models:

$$\frac{1}{\tau^{(j)}_{m_L m_M}} = \frac{6D_\perp}{b^{(j)}_{m_L m_M}} + m_M^2(D_\parallel - D_\perp) \tag{5}$$

$$\frac{1}{\tau^{(j)}_{m_L m_M}} = \frac{6D_\beta}{b^{(j)}_{m_L m_M}} + m_L^2(D_\alpha - D_\beta) \tag{6}$$

$$\frac{1}{\tau^{(j)}_{m_L m_M}} = \frac{6D_\beta}{b^{(j)}_{m_L m_M}} + m_L^2(D_\alpha - D_\beta) + \xi(m_M)D_\gamma \tag{7}$$

In Nordio's model, $D_\parallel$ and $D_\perp$ are the principal components of the diffusion tensor, diagonalized in a molecular frame, describing the molecular spinning and tumbling motions, respectively. In the *anisotropic viscosity* model, D_α and D_β correspond to the precession and tumbling motions of the

molecular long axis in the laboratory frame. The Volds' model is an extension of the *anisotropic viscosity* model, where the rotation of the molecule about its molecular long axis (γ-motion) is also taken into account and considered uncorrelated to α and β motions. $\xi(m_M)$ is $(1 - \delta m_M)$ or m_M^2 if the strong collision[15] or small step diffusion[14] models are used, respectively, for this motion. The coefficients $a^{(j)}_{m_L m_M}$, $b^{(j)}_{m_L m_M}$, and $c_{m_L m_M}$ have been calculated in ref 11 as a function of the principal order parameter for a Maier-Saupe potential.

For deuterium nuclei belonging to molecular fragments undergoing internal motions, a different formulation of J must be considered. Assuming internal rotations superimposed to overall molecular reorientations, one obtains

$$J_{m_L}(m_L\omega_0) = \frac{3\pi^2}{2}(\nu_q)^2 \sum_{m_M=-2}^{2} \sum_{m_R=-2}^{2} c_{m_L m_M}[d^2_{m_R 0}(\beta_{i,Q_i})]^2 [d^2_{m_M m_R}(\beta_{M,i})]^2 \sum_j a^{(j)}_{m_L m_M} \frac{(\tau^{(j)}_{m_L m_M})^{-1} + \xi(m_R)D_i}{(m_L\omega_0)^2 + [(\tau^{(j)}_{m_L m_M})^{-1} + \xi(m_R)D_i]^2} \tag{8}$$

where β_{i,Q_i} is the angle between the C−D bond and the axis about which the internal rotation takes place, $\beta_{M,i}$ is the angle between this axis and the molecular long axis, D_i is the diffusion coefficient relative to the internal rotation of the fragment, and $\xi(m_R)$ depends on the model chosen for this motion as previously seen for the γ-motion.

Theories exist for nematic and low-order smectic phases[20,21] which describe the contribution to the spectral densities of order director fluctuations, considered uncoupled to reorientational motions. Such contribution is predicted to be null for $J_2(2\omega_0)$ and to show a typical $\omega_0^{-1/2}$ frequency dependence for $J_1(\omega_0)$. The contribution to J_1 can be written following eq 9 for a deuterium undergoing overall molecular reorientations only, and eq 10 for a deuterium also experiencing internal motions

$$J_1^{DF}(\omega_0) = \frac{3\pi^2}{2}(\nu_q)^2[d^2_{00}(\beta_{M,Q_0})]^2(S_{zz})^2 T \frac{a_{DF}}{\sqrt{\omega_0}} \tag{9}$$

$$J_1^{DF}(\omega_0) = \frac{3\pi^2}{2}(\nu_q)^2[d^2_{00}(\beta_{i,Q_i})]^2[d^2_{00}(\beta_{M,i})]^2(S_{zz})^2 T \frac{a_{DF}}{\sqrt{\omega_0}} \tag{10}$$

where S_{ZZ} is the molecular order parameter and the factor a_{DF} depends on macroscopic parameters such as the average Frank elastic constant, the viscosity coefficient, and the autodiffusion translational constant.

THE SOFTWARE

CAGE is a package which adds new functions to the Mathematica environment. This allows exploitation of the functions already present in Mathematica; the environment chosen guarantees ease and flexibility in the data analysis, from the input of the data to the graphical representation of the results as well as in future improvements of the program.

Experimental data (relaxation times and order parameters, and corresponding temperatures and frequencies) and geometrical and magnetic parameters are input by means of dialogue windows; the data are stored in a text file, which can be accessed when required. To these data either a simulation or a fitting procedure can be applied. Models for overall and internal motions and order director fluctuations are chosen interactively from a list and spectral densities are consequently calculated following the equations reported in the theory section. The models currently implemented are the following: Nordio, *anisotropic viscosity*, and Vold for molecular overall reorientations; strong collision and small step diffusion for internal motions; and Pincus and Blinc for order director fluctuations. The data can be analyzed either individually at each experimental temperature and frequency (single point procedure) or all together, assuming an Arrhenius dependence of the diffusional coefficients with temperature (global target procedure).

The aim of the simulation procedure is to calculate the quantity Q, defined as

$$Q = \frac{\sum_i (J_i^{calc} - J_i^{exp})^2}{\sum_i (J_i^{exp})^2} \cdot 100 \tag{11}$$

where i runs from 1 to the total number of spectral densities determined experimentally.

This calculation can be either fully numerical, fixing all the motional parameters (diffusional or Arrhenius coefficients), or partially symbolic, fixing only some parameters and leaving the remaining ones as variables. The latter case is the most interesting since the trend of Q with some chosen motional parameters can be displayed through graphical functions of Mathematica (2-D or 3-D graphics, contour plots, etc.), thus simplifying the investigation of both Q minima and correlation among motional parameters.

The fitting procedure is based on the "NonlinearRegress" function of the "NonlinearFit" package of Mathematica: this minimizes the sum of squared residuals using a selectable algorithm (the default is the Levenberg−Marquardt one). However, when the number of parameters to be found by the fit is equal to the number of experimental spectral densities, the program automatically switches to a routine which attempts to find numerical solutions of the system of equations by means of the "FindRoot" Mathematica function using Newton's method. Before performing the fitting the user is asked to choose initial values of the fitting parameters and, possibly, to fix some of them.

After a fitting procedure or a simulation is completed, a command allows one to display calculated and experimental spectral densities and $J_1(\omega_0)/J_2(2\omega_0)$ ratios, absolute and relative residuals and diffusional coefficients against temperature.

CAGE runs on a PC (500 MHz Pentium II processor and 512 Mb RAM) running Mathematica version 4.0 and is freely available at request from the authors.

APPLICATIONS TO EXPERIMENTAL DATA

CAGE has been tested on experimental ^{2}H relaxation data collected in our research group on several deuterated calamitic liquid crystals; here three meaningful examples are reported.

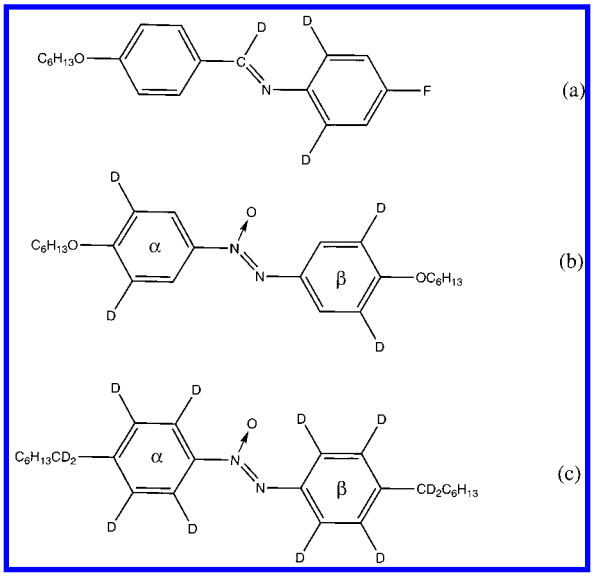

Figure 1. Molecular structures and labeling of the molecules: (a) FAB-OC6-d_3, (b) HL-d_4, and (c) HAB-d_{12}.

Single Point Analysis of ^{2}H T_{1Z} and T_{1Q} Relaxation Times of FAB-OC6-d_3. 4-Hexyloxybenzyliden-4′-fluoroaniline (FAB-OC6) is a calamitic mesogen showing nematic, smectic A, and smectic B liquid−crystalline phases.[24] The orientational ordering and dynamics of this mesogen in its liquid−crystalline phases have been studied previously by means of ^{2}H NMR spectroscopy and relaxation on the isotopomer FAB-OC6-d_3,[25] deuterated at the benzylidene methine group and at two positions of the aniline ring (see Figure 1a).

An interesting feature of this isotopomer is that the methine deuteron experiences overall molecular reorientations only, thus offering the possibility of testing models for molecular diffusion without the complication of internal motions. To this aim, the ^{2}H T_{1Z} and T_{1Q} relaxation times of FAB-OC6-d_3 in the nematic phase are here reinvestigated by means of the CAGE software analyzing at first the sole methine spectral densities in terms of Nordio's model and using the resulting diffusional coefficients as starting parameters in a successive analysis where aromatic spectral densities and internal phenyl ring motion, described through the strong collision model, are also taken into account. The same procedure was then repeated using the *anisotropic viscosity* model instead of Nordio's one.

In Figure 2a the values of Q as a function of $D_{\|}$ and $D_{\perp}$, computed starting from the experimental spectral densities of the sole methine deuteron in the nematic phase at 333.4 K, are reported. Geometrical, magnetic, and order parameters were taken from ref 25. As can be observed, Q shows a complex behavior in which two minima ($Q < 10^{-7}$) can be distinguished: the first is located at $D_{\|} \cong 9.8 \cdot 10^9$ s^{-1} and $D_{\perp} \cong 1.7 \cdot 10^8$ s^{-1} (see Figure 2b), and the second at $D_{\|} \cong 7.0 \cdot 10^9$ s^{-1} and $D_{\perp} \cong 8.9 \cdot 10^6$ s^{-1} (see Figure 2c). A region with relatively low Q values of about 0.25 is present for $D_{\|} \cong 6.0 \cdot 10^6$ s^{-1} and $D_{\perp} < 10^5$ s^{-1} (see Figure 2a). The same behavior of Q vs $D_{\|}$ and $D_{\perp}$ is shown throughout the nematic temperature range of FAB-OC6-d_3 implying the dependence of the solutions of the system on the starting values chosen for $D_{\|}$ and $D_{\perp}$.

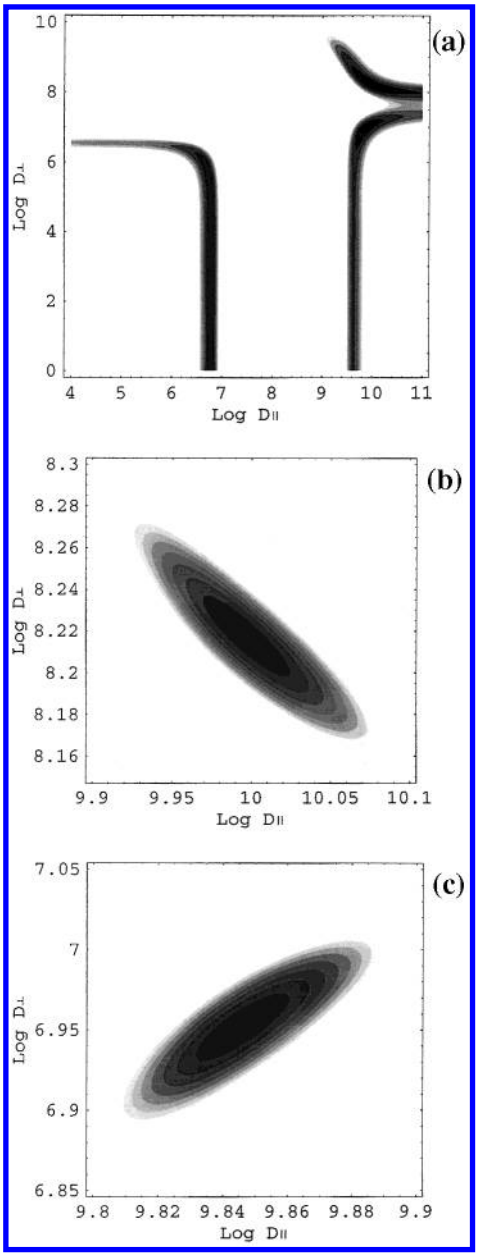

Figure 2. Q vs log $D_{\|}$ and log $D_{\perp}$ calculated for FAB-OC6-d_3 considering the sole methine spectral densities at 333.4 K using Nordio's model. (b) and (c) are an expansion of (a). The Q range is 0−20 in (a) and 0−0.1 in (b) and (c). Q values increase going from black to white.

When the relaxation data relative to the aromatic deuterons of FAB-OC6-d_3 are also considered, a fitting can be performed at each temperature since four experimental spectral densities are available from which three diffusion coefficients have to be calculated (namely $D_{\|}$ and $D_{\perp}$ for the molecular reorientation and D_R for the internal rotation of the aromatic ring, see eqs 4, 5, and 8). If the $D_{\|}$ and $D_{\perp}$ values giving Q minima in the simulation procedure applied to the sole methine spectral densities (see Figure 2 (parts b and c)) are taken for describing the overall molecular motions, optimum values for D_R can be estimated in a simulation procedure applied to the whole ensemble of experimental data. In Figure 3 the results obtained at $T =$ 333.4 K are reported. The two sets of three diffusion coefficients so found can be thus introduced as starting values in a fitting procedure to optimize $D_{\|}$, $D_{\perp}$, and D_R. The results,

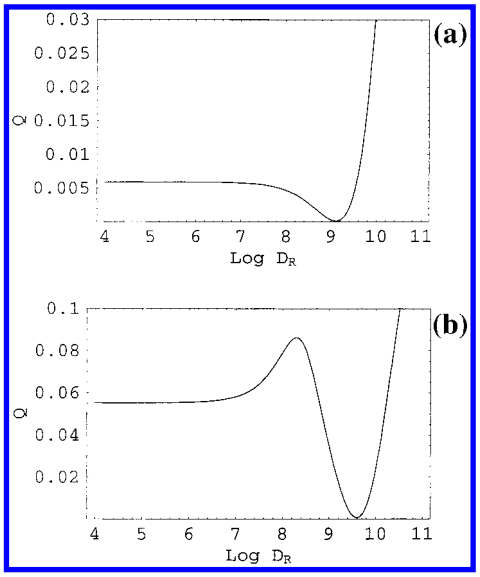

Figure 3. Q vs log D_R calculated for FAB-OC6-d_3 considering the methine and aromatic spectral densities at 333.4 K using Nordio's model for overall motions and superimposed strong collision model for phenyl ring rotation with (a) $D_\perp = 1.7 \cdot 10^8$ s^{-1} and $D_\parallel = 9.8 \cdot 10^9$ s^{-1}, (b) $D_\perp = 8.9 \cdot 10^6$ s^{-1}, and $D_\parallel = 7.0 \cdot 10^9$ s^{-1}.

Table 1. Results of the Analysis of Methine and Aromatic Spectral Densities of FAB-OC6-d_3 at 333.4 K in Terms of Either Nordio's or *Anisotropic Viscosity* Models Superimposed to Strong Collision Model for the Rotation of the Phenyl Ring about Its *Para* Axis

$D_\parallel$ (s^{-1})	$D_\perp$ (s^{-1})	D_R (s^{-1})	Q
Nordio's Model			
$(1.02 \pm 0.05) \cdot 10^{10}$	$(1.62 \pm 0.06) \cdot 10^8$	$(1.01 \pm 0.35) \cdot 10^9$	$6.5 \cdot 10^{-3}$
$(7.21 \pm 0.63) \cdot 10^9$	$(9.3 \pm 1.1) \cdot 10^6$	$(3.80 \pm 0.80) \cdot 10^9$	$5.6 \cdot 10^{-2}$
D_α (s^{-1})	D_β (s^{-1})	D_R (s^{-1})	Q
Anisotropic Viscosity Model			
$(3.56 \pm 0.13) \cdot 10^9$	$(6.42 \pm 0.50) \cdot 10^8$	$(4.90 \pm 0.34) \cdot 10^9$	$1.9 \cdot 10^{-2}$
$(4.8 \pm 2.1) \cdot 10^6$	$(1.61 \pm 0.64) \cdot 10^6$	$(1.46 \pm 0.40) \cdot 10^{10}$	1.9

shown in Table 1, indicate that fittings of good quality can be obtained in the two cases, with final values of the coefficients depending on the starting ones.

The same data treatment (i.e. simulation of methine spectral densities, fitting of methine plus aromatic spectral densities after a prescreening of the diffusion coefficients by means of a simulation) has been performed on the spectral densities measured at different temperatures in the nematic phase of FAB-OC6-d_3 in terms of the *anisotropic viscosity* model. In this case, two minima of Q as a function of D_α and D_β are found taking into account the sole methine spectral densities at each investigated temperature. At $T =$ 333.4 K, the first minimum is located at $D_\alpha \cong 3.6 \cdot 10^9$ s^{-1} and $D_\beta \cong 6.2 \cdot 10^8$ s^{-1}, and the second one at $D_\alpha \cong 4.8 \cdot 10^6$ s^{-1} and $D_\beta \cong 1.6 \cdot 10^6$ s^{-1} (see Figure 4). When the whole set of spectral densities is considered and the internal motion of the phenyl ring is introduced in the model, fittings of different quality are obtained (see Table 1), a remarkably better reproduction of experimental data being achieved in the first case.

The different behavior of the two models is in agreement with the relatively low order parameter at the temperature here investigated ($S_{ZZ} = 0.37$). However, since $D_\perp$ and D_β describe the same tumbling motion, the results obtained applying the *anisotropic viscosity* model confirms that,

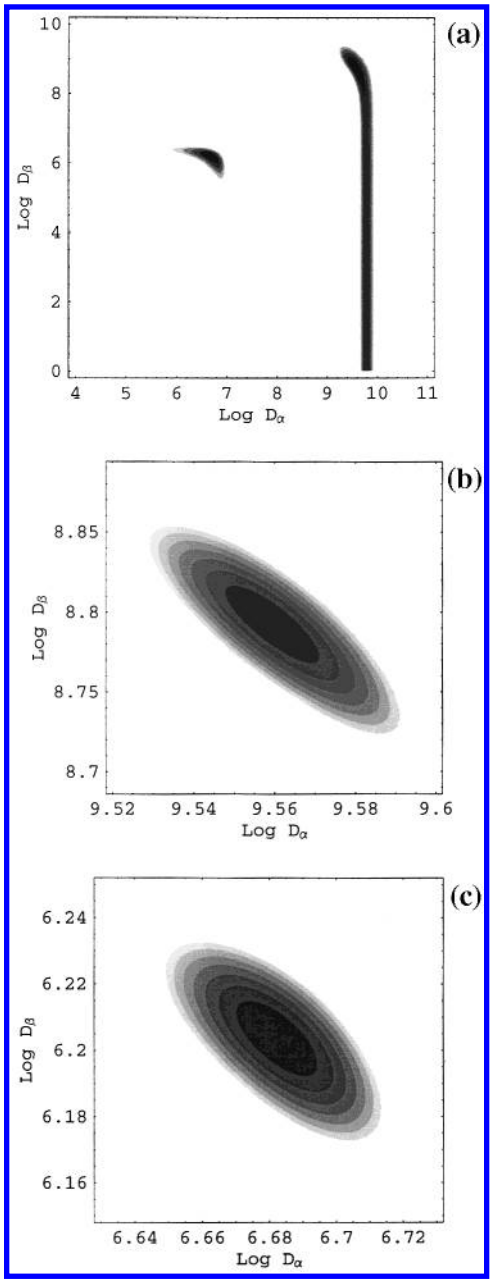

Figure 4. Q vs log D_α and log D_β calculated for FAB-OC6-d_3 considering the sole methine spectral densities at 333.4 K using the *anisotropic viscosity* model. (b) and (c) are an expansion of (a). The Q range is 0−15 in (a) and 0−0.1 in (b) and (c).

between the two solutions obtained by Nordio's model, that with the higher $D_\perp$ value is to be preferred.

Global Target Analysis of ^{2}H T_{1Z} and T_{1Q} Relaxation Times of HL-d_4. 4,4′-Bis(hexyloxy)azoxybenzene (HL) is a calamitic mesogen showing a nematic phase over a temperature range of 55 degrees.[26] Orientational order[27] and dynamics[28] of HL have been previously studied by means of ^{2}H NMR on its isotopomer HL-d_4 partially deuterated on the two phenyl rings (see Figure 1b).

The dynamics of HL-d_4 is here reinvestigated to give an example of the application of the global target procedure using the magnetic, geometric, and order parameters reported in refs 27 and 28. In fact, on one side the presence of deuterons on two different molecular moieties, both undergoing internal motions, complicates the application of a single point approach, and, on the other side, the relatively broad

nematic range improves the reliability of the dynamic parameters extracted from a global target procedure.

However, the achievement of physically meaningful results from a global fitting is not straightforward for at least two reasons. First, the equations involved in the calculations are extraordinarily complicated, showing a nontrivial dependence on the individual fitting parameters. Second, the introduction of temperature dependence for the diffusional coefficients implies not only a doubling of the number of fitting parameters (eight, in the present case) but also a strong correlation between each preexponential coefficient and the corresponding activation energy, which could be partially removed for experimental data over a very broad temperature range. As a consequence, the choice of initial values of the fitting parameters strongly affects the final results, and sometimes it is necessary to keep some parameters fixed at chosen values to achieve convergence.

In the present case, the use of the simulation routines included in CAGE allowed us to select suitable starting values for the fitting parameters as well as to investigate the possible presence of multiple solutions. An example illustrating the complexity of the problem is given by the dependence of the *Q* factor on the diffusional coefficients for the internal motions of each phenyl ring, computed at fixed values of the diffusional coefficients for overall molecular motions ($D_{\|}$ and $D_{\perp}$ using Nordio's model) taking into account the spectral densities of one kind of deuteron at a time. It can be seen in Figure 5 that small changes in $D_{\|}$ cause dramatic changes of *Q* as a function of $D_{R\alpha}$, the diffusion coefficient for the α phenyl ring rotation, described in terms of the strong collision model. In particular, sharp minima of *Q* always occur for values of $D_{R\alpha}$ between 10^8 and 10^{10} s^{-1} (see Figure 5 (parts a and b)), but a completely different trend, with *Q* decreasing by lowering $D_{R\alpha}$, is observed for certain couples of $D_{\|}$ and $D_{\perp}$ values (see Figure 5c). This behavior makes it difficult to find the global minimum in a fitting procedure and can bring to mathematically acceptable but physically unreasonable results (for instance $D_{R\alpha} = 0$) when starting values of the parameters are not suitably chosen. In this case, $D_{R\alpha}$ can be constrained reliably between 10^8 and 10^{10} s^{-1}. Simulations carried out by fixing $D_{R\alpha}$ at several values within this range revealed that two similarly good solutions can be found for each data point with $D_{\|} \cong 10^{10}$ s^{-1} and $D_{\perp} \cong 3 \cdot 10^7$ s^{-1} and $D_{\|} \cong 10^{10}$ s^{-1} and $D_{\perp} \cong 7 \cdot 10^5$ s^{-1}. Similar results were obtained for the β phenyl ring.

Initial values of the fitting parameters compatible with these two minima were used in a global fitting procedure carried out using all the available experimental spectral densities (see Figure 6a): accordingly, two sets of results were found (see Figure 6 (parts b and c)) giving comparably good reproductions of the experimental spectral densities. In Figure 6a the calculated spectral densities corresponding to diffusional coefficients of Figure 6b are reported: substantially identical spectral densities are obtained for diffusional coefficients of Figure 6c. The reason we speak in terms of "sets of results" rather than "results" is that the strong correlation between activation energies and preexponential coefficients cannot be completely removed in the temperature range here explored, thus leaving a remarkable uncertainty in the determination of their individual values.

Global Target Analysis of ^{2}H T_{1Z} and T_{1Q} Relaxation Times of HAB-d$_{12}$ at Two Different Larmor Frequencies.

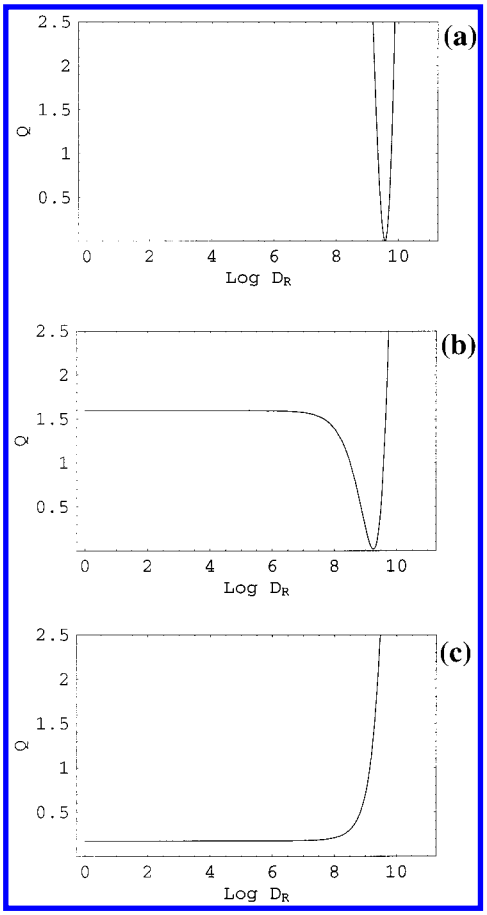

Figure 5. *Q* vs log D_R calculated for HL-d$_4$ considering the spectral densities of ring α at 374 K using Nordio's model for overall motions and superimposed strong collision model for phenyl ring rotation with $D_{\perp} = 4.0 \cdot 10^7$ s^{-1} and (a) $D_{\|} = 6.3 \cdot 10^9$ s^{-1}, (b) $D_{\|} = 7.9 \cdot 10^9$ s^{-1}, and (c) $D_{\|} = 1.0 \cdot 10^{10}$ s^{-1}.

4,4′-Bis(heptyl)azoxybenzene (HAB) is a calamitic mesogen showing a nematic phase between 326.5 and 344.5 K and a smectic A phase between 307 and 326.5 K.[29] ^{2}H T_{1Z} and T_{1Q} relaxation times were previously measured between 309 and 337 K on its isotopomer HAB-d$_{12}$ deuterated on both the phenyl rings and on the first methylene group of the two chains (see Figure 1c) at two different frequencies, namely 46.04 and 10 MHz, and analyzed by means of a single point procedure.[30]

Here, a global target procedure is applied to the whole set of relaxation data obtained in the smectic A phase (two pairs of spectral densities for the aromatic and one for the methylene deuterons at each temperature and frequency, shown in Figure 7 (parts a and b)), taking geometrical, magnetic, and order parameters from ref 31. The availability of spectral densities at two different frequencies, in combination with the presence of deuterons in the aliphatic chains, indeed allows quantitative information on order director fluctuations to be obtained. In fact, the typical $\omega_0^{-1/2}$ dependence of $J_1(\omega_0)$ is overshadowed, for aromatic deuterons, by the term $d^2_{00}(\beta_{i,Q_i}) = (3\cos^2\beta_{i,Q_i} - 1)/2$, almost vanishing when $\beta_{i,Q_i} \approx 60°$. However, the large size of the experimental data set makes the application of a global target procedure even more complicated than in the case of HL-d$_4$. Therefore, to fully explore the possible solutions of the problem, it is necessary to follow several indermediate steps before attempting an analysis of the whole data set. In

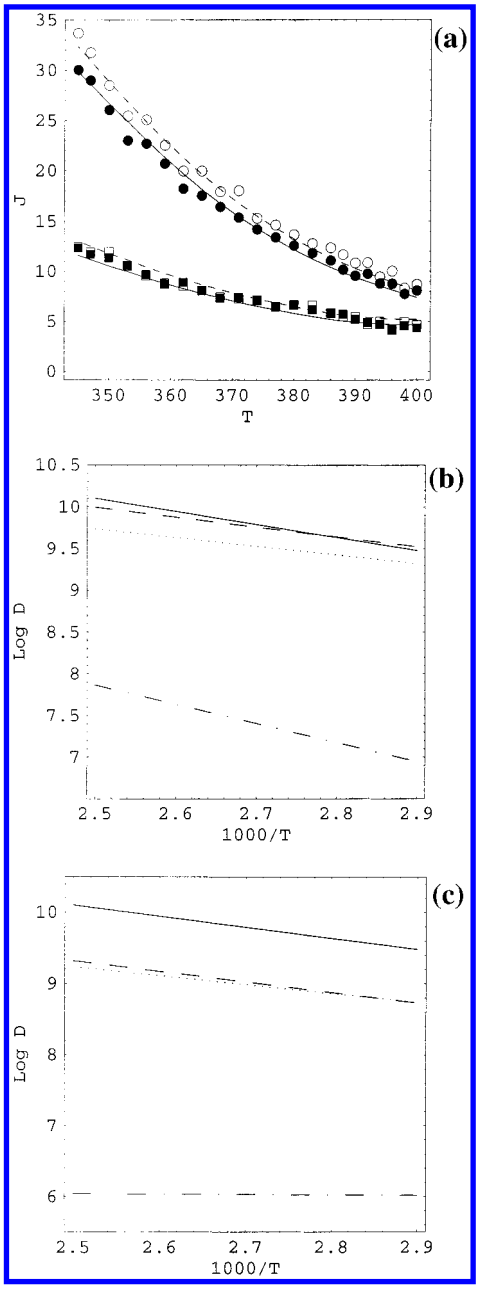

Figure 6. (a) Experimental (symbols) and calculated (lines) spectral densities (s^{-1}) of HL-d_4 in the nematic phase vs T (K). Circles and squares represent experimental $J_1(\omega_0)$ and $J_2(2\omega_0)$, respectively. Filled symbols and solid lines refer to α aromatic deuterons; open symbols and dashed lines refer to β aromatic deuterons. (b)−(c) Diffusional coefficients (s^{-1}) vs 1000/T (K^{-1}): solid, dot−dashed, dashed, and dotted lines indicate $D_{\|}$, $D_{\perp}$, $D_{R\alpha}$, and $D_{R\beta}$, respectively.

particular, we first used the sole spectral densities of aromatic deuterons to determine the dynamic parameters for the molecular overall motions. To this aim, in agreement with what previously done for HL-d_4, we applied a single point simulation procedure to the spectral densities of the deuterons of each phenyl ring and then a global fitting procedure to the whole set of spectral densities of the deuterons of both phenyl rings at both frequencies. Using Nordio's model for the overall molecular motions and the strong collision model for phenyl ring rotations about their *para* axes (described by $D_{R\alpha}$ and $D_{R\beta}$), we found two sets of solutions with comparable Q values, one with $D_{\|} \cong 2.5 \cdot 10^9\ s^{-1}$, $D_{\perp} \cong 3.2 \cdot 10^8\ s^{-1}$, $D_{R\alpha} \cong 1.6 \cdot 10^9\ s^{-1}$, and $D_{R\beta} \cong 7.9 \cdot 10^8\ s^{-1}$, the other with $D_{\|} \cong 3.2 \cdot 10^9\ s^{-1}$, $D_{\perp} \cong 2.5 \cdot 10^6\ s^{-1}$, $D_{R\alpha} \cong 1.3 \cdot 10^9\ s^{-1}$, and $D_{R\beta} \cong 1.3 \cdot 10^9\ s^{-1}$. These results have been then introduced as starting values in a global fitting where also spectral densities of methylene deuterons at both frequencies were included, strong collision model was used for methylene group reorientations (described by D_{CD2}), and order director fluctuations (see eq 10) were taken into account. A good fitting was obtained in both cases. In Figure 7 (parts a and b) experimental and calculated spectral densities for one case are reported (essentially identical values are obtained for the other case); the diffusional coefficients found in the two cases are shown in Figure 7 (parts c and d). a_{DF} values of $(1.14 \pm 0.05) \cdot 10^{-8}$ and $(1.29 \pm 0.06) \cdot 10^{-8}\ K^{-1}s^{1/2}\ rad^{-3/2}$ were found, corresponding to contributions to J_1 of about 2−5% and 4−10% for aromatic deuterons at 46.04 and 10 MHz, respectively, and of about 54−64% and 56−68% for methylene deuterons at 46.04 and 10 MHz, respectively.

CONCLUSIONS

We have presented a Mathematica software package (CAGE) written for the analysis of spectral densities in liquid crystals, obtained from ^2H Zeeman and quadrupolar spin−lattice relaxation measurements, in terms of the most commonly used models for overall, internal, and collective motions. Applications of CAGE to three experimental relaxation data sets of different complexity have been reported with the aim of illustrating the features of this software. In the first example the single point procedure was applied to FAB-OC6-d_3 deuterated on two different fragments, one of which does not experience internal motions, focusing on the comparison between models describing overall molecular motions. In the second example the global target approach was used for analyzing the spectral densities of the aromatic deuterons collected throughout the nematic phase of HL-d_4. In the third case we dealt with the global target analysis of spectral densities of both aromatic and aliphatic deuterons of HAB-d_{12} measured at two different frequencies throughout its smectic A phase, with particular attention to the contribution of order director fluctuations to the relaxation.

In these three examples, which are representative of most cases reported in the literature on deuterium relaxation in liquid crystals, the CAGE software highlighted that achieving unambiguous physically meaningful results is not straightforward. This occurs either because of the strong correlation between activation energies and preexponential coefficients in the Arrhenius equation considered in the global target procedure or because of the presence of different sets of dynamic parameters giving comparably good fittings of experimental data. If on one side the parameter correlation can be considered intrinsic in the Arrhenius equation, the problem of multiple solutions is here explicitly discussed for the first time. To this regard, a step by step approach, including simulations and fittings on partial sets of data suitably selected, is essential in order to obtain results independent from the choice of good starting values for the parameters to be optimized, especially when very complex cases involving several deuterons, temperatures, and frequencies have to be analyzed. The CAGE software was to cope with this problem, even though the choice among several physically acceptable solutions could require further experi-

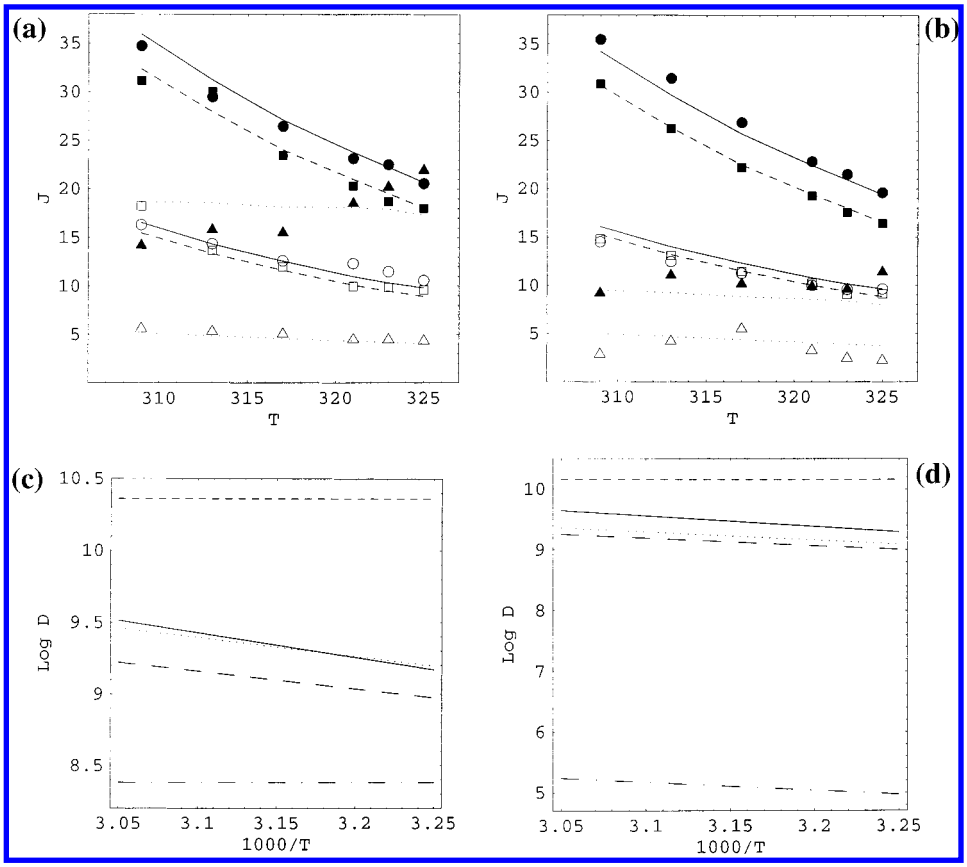

Figure 7. Experimental (symbols) and calculated (lines) spectral densities (s^{-1}) of HAB-d_{12} in the smectic A phase vs T (K) at (a) 10 MHz and (b) 46.04 MHz. Filled and open symbols represent experimental $J_1(\omega_0)$ and $J_2(2\omega_0)$, respectively. Squares and dashed lines refer to α aromatic deuterons; circles and solid lines refer to β aromatic deuterons; triangles and dotted lines refer to methylene deuterons. (c)−(d) Diffusional coefficients (s^{-1}) vs 1000/T (K^{-1}): solid, dot−dashed, long-dashed, dotted, and short-dashed lines indicate $D_{\|}$, $D_{\perp}$, $D_{R\alpha}$, $D_{R\beta}$, and D_{CD2}, respectively.

mental efforts (deuteration of more molecular moieties or measurement of frequency and orientation dependent spectral densities) or comparison with findings of different techniques (e.g. dielectric relaxation).

Additional investigations can be performed with CAGE; for instance it could be used to analyze the influence of magnetic and geometric parameters on the quality of results or on the optimized dynamic parameters' values as well as to compare the adequacy of different theoretical models for overall (i.e., Nordio's, *anisotropic viscosity*, Volds' models) and internal (i.e., strong collisions and small step models) motions in reproducing the experimental data. Further developments of CAGE, made easy because of its modular nature, are in progress aimed on one side to add new theoretical models for the description of overall (e.g. diffusion in a cone) and internal motions (e.g. Heaton and Kothe model for the intramolecular phenyl ring dynamics) and on the other side to analyze variable angle relaxation data.

We hope that the results here presented will stimulate a critical reinvestigation of other data already reported in the literature and that further theoretical efforts will be made to improve the interpretation of deuterium spin−lattice relaxation times in terms of motional parameters describing the dynamics of liquid crystals.

ACKNOWLEDGMENT

The authors thank Dr. C. Forte and Prof. C. A. Veracini for the helpful discussions.

REFERENCES AND NOTES

(1) Moro, G.; Segre, U.; Nordio, P. L. In *Nuclear Magnetic Resonance of Liquid Crystals*; Emsley, J. W., Ed.; D. Reidel: Dordrecht, 1985; Chapter 9, pp 207−230.
(2) Vold, R. R. In *Nuclear Magnetic Resonance of Liquid Crystals*; Emsley, J. W. Ed.; D. Reidel: Dordrecht, 1985; Chapter 11, pp 253−288.
(3) *The Molecular Dynamics of Liquid Crystals*; Luckhurst, G. R., Veracini, C. A., Eds.; Kluwer Academic: Dordrecht, 1994.
(4) Dong, R. Y. *Nuclear Magnetic Resonance of Liquid Crystals*; Springer-Verlag: New York, 1994.
(5) Jeener, J.; Broekaert, P. NMR in solids; thermodynamic effects of a pair of r.f. pulses. *Phys. Rev.* **1967**, *157*, 232−240.
(6) Wimperis, S. Broadband and narrowband composite excitation sequences. *J. Magn. Reson.* **1990**, *86*, 46−59.
(7) Geppi, M.; Forte, C. The SPORT-NMR software: a tool for determining relaxation times in unresolved NMR spectra. *J. Magn. Reson.* **1999**, *137*, 177−185.
(8) Wang, C. C.; Pecora, R. Time-correlation functions for restricted rotational diffusion. *J. Chem. Phys.* **1980**, *72*, 5333−5340.
(9) Nordio, P. L.; Busolin, P. Electron spin resonance line shapes in partially oriented systems. *J. Chem. Phys.* **1971**, *55*, 5485−5490. Nordio, P. L.; Rigatti, G.; Segre, U. Spin relaxation in nematic solvents. *J. Chem. Phys.* **1972**, *56*, 2117−2123.
(10) Polnaszek, C. F.; Bruno, G. V.; Freed, J. H. ESR line shapes in the slow-motional region: anisotropic liquids. *J. Chem. Phys.* **1975**, *58*, 3185−3199; Polnaszek, C. F.; Freed, J. H. Electron spin resonance studies of anisotropic ordering, spin relaxation, and slow tumbling in liquid crystalline solvents. *J. Phys. Chem.* **1975**, *79*, 2283−2306.
(11) Vold, R. R.; Vold, R. L. Nuclear spin relaxation and molecular dynamics in ordered systems: models for molecular reorientation in thermotropic liquid crystals. *J. Chem. Phys.* **1988**, *88*, 1443−1457.
(12) Tarroni, R.; Zannoni, C. On the rotational diffusion of asymmetric molecules in liquid crystals. *J. Chem. Phys.* **1991**, *95*, 4550−4564.
(13) Berggren, E.; Tarroni, R.; Zannoni, C. Rotational diffusion of uniaxial probes in biaxial liquid crystal phases. *J. Chem. Phys.* **1993**, *99*, 6180−6200.

(14) Woessner, D. E. Spin relaxation processes in a two-proton system undergoing anisotropic reorientation. *J. Chem. Phys.* **1962**, *36*, 1−4. Dong, R. Y. Molecular dynamics and spectral density determination in liquid crystals. *Mol. Cryst. Liq. Cryst.* **1986**, *141*, 349−359.
(15) Beckmann, P. A.; Emsley, J. W.; Luckurst, G. R.; Turner, D. L. Nuclear spin-lattice relaxation rates in liquid crystals. Results for deuterons in specifically deuteriated 4-*n*-pentyl-4′-cyano biphenyl in both nematic and isotropic phases. *Mol. Phys.* **1986**, *59*, 97−125.
(16) Heaton, N. J.; Kothe, G. Phenyl ring dynamics and chain reorientation in liquid crystal polymers: a deuteron spin relaxation study. *J. Chem. Phys.* **1998**, *108*, 8199−8213.
(17) Tsutsumi, A. Nuclear magnetic spin relaxation of a spin-pair undergoing reorientations by jumping among unequivalent sites. *Mol. Phys.* **1979**, *37*, 111−127. London, R. E.; Avitabile, J. Calculation of ^{13}C relaxation times and Nuclear Overhauser Enhancements in a hydrocarbon chain undergoing gauche−trans isomerism. *J. Am. Chem. Soc.* **1977**, *99*, 7765−7776. London, R. E.; Avitabile, J. Calculated ^{13}C NMR relaxation parameters for a restricted internal diffusion model. Application to methionine relaxation in dihydrofolate reductase. *J. Am. Chem. Soc.* **1978**, *100*, 7159−7165.
(18) Wallach, D. Effect of internal rotation on angular correlation functions. *J. Chem. Phys.* **1967**, *47*, 5258−5268.
(19) Wittebort, R. J.; Szabo, A. Theory of NMR relaxation in macromolecules: restricted diffusion and jump models for multiple internal rotations in amino acid side chains. *J. Chem. Phys.* **1978**, *69*, 1722−1736. Dong, R. Y.; Richards, G. M. Modeling of correlated internal motions and deuteron spin relaxation in liquid crystals. *Chem. Phys. Lett.* **1990**, *171*, 389−393.
(20) Pincus, P. Nuclear relaxation in a nematic liquid crystal. *Solid St. Commun.* **1969**, *7*, 415−418.
(21) Blinc, R.; Hogenboom, D.; O'Reilly, D.; Peterson, E. Spin relaxation and self diffusion in liquid crystals. *Phys. Rev. Lett.* **1969**, *23*, 969−972.
(22) Dong, R. Y. Global analysis of deuteron relaxation data in MBBA. *Mol. Phys.* **1996**, *88*, 979−985.
(23) Trademark of Wolfram Research Inc.
(24) Gandolfo, C.; Grasso, D.; Buemi, G.; Torquati, G. Phase transitions and structural studies of p-*n*-alkoxybenzyliden-p′-fluoro-anilines. *Nuovo Cim. D* **1988**, *10*, 1363−1371.
(25) Calucci, L.; Geppi, M.; Veracini, C. A.; Forte, C.; Gandolfo, C. A ^2H NMR study of orientational order and spin relaxation in the mesogen p-hexyloxybenzylidene-p′-fluoroaniline. *Mol. Cryst. Liq. Cryst.* **1997**, *303*, 415−429.
(26) Chow, L. C.; Martire, D. E. Thermodynamics of solutions with liquid crystal solvents. II. Surface effects with nematogenic compounds. *J. Phys. Chem.* **1969**, *73*, 1127−1132.
(27) Calucci, L; Catalano, D.; Ghedini, M.; Jones, N. L.; Pucci, D.; Veracini, C. A. ^2H NMR study of the cyclopalladated 4,4′-bis(hexyloxy)-azoxybenzene, a complex showing a nematic phase. *Mol. Cryst. Liq. Cryst.* **1996**, *290*, 87−98.
(28) Calucci, L.; Forte, C.; Geppi, M.; Veracini, C. A. Dynamics of liquid crystals by means of ^2H NMR: a comparison between 4,4′-bis-(hexyloxy)azoxybenzene and the derivative Pd(II) complex Azpac. *Z. Naturforsch.* **1998**, *53a*, 427−435.
(29) Emsley, J. W.; Hashim, R.; Luckurst, G. R.; Rumbles, G. N.; Viloria, F. R. The Saupe ordering matrices for solutes in uniaxial liquid crystals. Experiment and theory. *Mol. Phys.* **1983**, *49*, 1321−1335.
(30) Forte, C.; Geppi, M.; Veracini, C. A. Study of the molecular dynamics from deuterium Zeeman and quadrupolar NMR Relaxation of 4,4′-di-*n*-heptylazoxybenzene in the nematic and smectic A phases. *Z. Naturforsch.* **1994**, *49a*, 311−319.
(31) Catalano, D.; Forte, C.; Veracini, C. A.; Emsley, J. W.; Shilstone, G. N. Orientational order in nematic and smectic A phases of three closely related compounds: 4,4′-di-*n*-heptylazobenzene, 4,4′-di-*n*-heptyl- and 4,4′-di-*n*-octylazoxybenzene. *Liq. Cryst.* **1987**, *2*, 345−355.

CI000169W